



Photocatalytic treatment of aqueous solutions at high dye concentration using praseodymium-doped ZnO catalysts

Vincenzo Vaiano*, Mariantonietta Matarangolo, Olga Sacco, Diana Sannino

Department of Industrial Engineering, University of Salerno, via Giovanni Paolo II, 132, 84084 Fisciano, SA, Italy



ARTICLE INFO

Article history:

Received in revised form 23 February 2017

Accepted 1 March 2017

Available online 16 March 2017

Keywords:

Pr-doped ZnO

Photocatalysis

High dye concentration

UV or visible irradiation

ABSTRACT

In this work the photocatalytic activity of Pr-doped ZnO (Pr-ZnO) photocatalysts has been addressed for the first time in the treatment of aqueous solutions at high concentration of organic dyes under UV or visible light irradiation. Pr-ZnO photocatalysts were prepared by a precipitation method. The catalysts have been characterized by different techniques such as X-ray diffraction (XRD), UV-Vis diffuse reflectance (UV-Vis DRS) and Raman spectroscopy. XRD results showed that Pr^{3+} ions were successfully incorporated into the ZnO lattice. UV-Vis DRS spectra evidenced that Pr-ZnO samples present band-gap values of about 3.0 eV, lower than undoped ZnO (3.3 eV). The efficiency of photocatalysts has been tested in the photocatalytic removal of the azo dye Eriochrome Black T (EBT) under UV or visible light irradiation. The experimental results showed that the values of discoloration and mineralization rate are correlated to the Pr doping level, evidencing that the optimal loading of Pr in the ZnO structure is 0.46 mol%. The influence of process parameters (catalyst dosage, initial dye concentration and presence of carbonate ions) on the extent of photocatalytic performances has been investigated. The efficiency of the optimized photocatalyst was also evaluated in the photocatalytic treatment of aqueous solutions containing the triphenylmethane Patent Blue V (PB) dye and in the treatment of a solution containing simultaneously the two selected dyes (EBT and PB). Photocatalytic activity tests in presence of ion scavengers (carbonate ions) showed that the formulated Pr-ZnO photocatalyst is not subjected to deactivation phenomena. At last, a very interesting result was observed for the treatment of a real wastewater containing Basic Red 51 dye, showing that the complete discoloration and mineralization was achieved.

© 2017 Elsevier B.V. All rights reserved.

1. Introduction

Organic dyes are the major class of pollutants in the wastewater coming from textile, paper printing, rubber and plastic manufacturing processes, wood and silk industries. As it is well known, dyes used in these industrial activities are toxic and carcinogenic and for this reason, they represent a serious problem for the human and animal health [1]. It is estimated that about 12% of synthetic textile dyes (such as Red indigo, Red 120, Rhodamine B, Methylene Blue, Eriochrome Black T) used each year, are lost during operations machining, and 20% of these lost dyes it is found in industrial wastewater and therefore in the environment. With regard to the removal processes of organic dyes, the conventional treatments like biological, physical and chemical processes (adsorption or coagulation) have a low removal efficiency because dyes are stable to the light and to the oxidizing agent [2].

In this sense, the heterogeneous photocatalysis is a promising approach [3–10]. Photocatalysis has been studied in the decomposition of a variety of undesirable organic pollutants and seems to be an achievable process for the degradation of dyes in water courses by using solar or artificial light illumination [11–16]. Although most of the literature studies are focused on the use of TiO_2 , it must be considered that this photocatalyst has several limitations such as deactivation in the presence of ions scavengers in solution as well as a low degradation kinetic in the presence of a high content of dyes in aqueous samples [17]. These aspects determine the still low use of TiO_2 in real-scale processes.

As alternative to TiO_2 , ZnO is one among the semiconductors better suited to photocatalytic processes demonstrating a degradation efficiency comparable to TiO_2 [18–20] without any deactivation in the presence of ions scavengers [21,22]. Many studies have been made to investigate ZnO mediated photocatalytic degradation of organic dyes, such as Congo Red, Rhodamine B, Eriochrome Black T, Methylene Blue, Eosin Y, Reactive Orange 16 and Reactive Red 180 [23–26]. However, an important aspect to underline is that the solutions most studied in the current scientific

* Corresponding author. Tel.: +39 089964006.

E-mail address: vvaiano@unisa.it (V. Vaiano).

literature, have concentrations of dyes in the range of 20–60 mg L⁻¹ [26–28]. Generally, dye concentrations, present in wastewater, varied from very low to high concentrations (5 to 1500 mg L⁻¹) that lead to color dye effluents causing toxicity, including carcinogenic and mutagenic effects in biological ecosystems [29].

The problem of treating aqueous solutions with a high concentration of dyes by means of photocatalysis is correlated to the photonic limitation; in fact, with high dye concentration, the light radiation may have difficulties to irradiate the entire volume of solution.

To enhance the photocatalytic activity, the doping of semiconductors is demonstrated to be a promising method because it is effective, convenient and easy. The scientific literature reports the doping of ZnO with metal ions such as Cu, Ag, Co and Fe [30–32] showing an increase of performances compared to undoped ZnO [33,34]. However, in some cases, a decrease of the photocatalytic activities is obtained [35]. With the aim to consider alternative dopants different from noble and transition metals, it should be considered that ZnO is a good host for incorporating chemical elements belonging to the lanthanide group, such as praseodymium (Pr) with the production of defects such as oxygen deficiency [36]. For this reason, in this work it was investigated the photocatalytic activity of Pr-doped ZnO catalysts (at different content of doping) for the treatment of aqueous solutions with a high concentration of dyes, such as Eriochrome Black T (EBT) and Patent Blue V (PB).

EBT is one of the most important azo-dye used for dyeing silk, wool, nylon while PB is a recognized dye in food industry [36,37]. These two dyes are difficult to remove with conventional treatments [38].

At our knowledge, this is the first paper reporting the use of ZnO doped with Pr in a photocatalytic system for the removal of different class of dyes.

2. Experimental

2.1. Preparation of dye solutions

A defined amount of EBT (Sigma-Aldrich) was dissolved in 1 L of distilled water to obtain different dye concentration. In this way, the following EBT solutions were prepared: 50, 100, 150 and 300 mg L⁻¹.

In the same manner, it was prepared a solution with different amount of PB dye (Sigma-Aldrich); in particular, the PB concentrations were: 10, 50 and 100 mg L⁻¹.

At last, it was prepared a solution containing simultaneously the two dyes with the concentration of 50 mg L⁻¹ both.

2.2. Experimental: Photocatalysts preparation

2.2.1. Undoped ZnO catalyst

Undoped ZnO catalyst was prepared by the precipitation method starting from 8 g of ZnSO₄ (Aldrich, 99%) dissolved in 50 mL of distilled water and then by the slow addition of an aqueous solution obtained dissolving 4 g of NaOH (Aldrich, 99%) in 25 mL of distilled water at room temperature. Afterward, the generated precipitate was centrifuged, washed and calcined at 450 °C for 30 min.

2.2.2. Praseodymium doped ZnO

Pr(NO₃)₃·6H₂O (Aldrich 99%) was used in the doping procedure. Different amounts of Pr(NO₃)₃·6H₂O were dissolved into the solution of ZnSO₄ before to induce the precipitation with NaOH. The obtained precipitate was centrifuged, washed and calcined at 450 °C for 30 min.

All the photocatalysts synthesized were listed in Table 1.

The Pr nominal loading was expressed as molar percentage, and it was evaluated through the following equation:

$$\% \text{molPr} = \frac{n_{\text{Pr}}}{n_{\text{Zn}}} \cdot 100 \quad (1)$$

where n_{Pr} is the number of moles of Pr(NO₃)₃·6H₂O used in the synthesis; n_{Zn} is the number of moles of ZnSO₄ used in the synthesis.

2.2.3. Characterization of the photocatalysts

All the synthesized catalysts were characterized using different techniques.

The specific surface area (SSA) analysis was performed by BET method using N₂ adsorption with a Costech Sorptometer 1042 after a pretreatment at 150 °C for 30 min in He flow (99.9990%). Total Pr loading of the samples were determined by X-ray fluorescence spectrometry (XRF) in a thermoFischer ARL QUANT'X EDXRF spectrometer equipped with a rhodium standard tube as the source of radiation and with Si-Li drifted crystal detector. The crystal phases of ZnO based photocatalysts were determined by XRD analysis carried out on Brucker D8 diffractometer and the crystallite sizes were calculated from using the Scherrer equation. The morphology of the prepared samples was examined using a scanning electron microscope (SEM, VegaTescan LMH II).

UV-Vis reflectance spectra were recorded with a PerkinElmer spectrometer Lambda 35 while band-gaps values were calculated from the corresponding Kubelka-Munk functions, $F(R\infty)$, which are proportional to the absorption of radiation by plotting $(F(R\infty) \times h\nu)^2$ against $h\nu$. Raman spectroscopy studies were carried out on a Dispersive MicroRaman spectrometer (Invia, Renishaw) with a 514 nm diode-laser in the range 150–750 cm⁻¹.

2.3. Experimental: evaluation of photocatalytic activity

The photocatalytic experiments were carried out with a Pyrex cylindrical reactor (ID = 2.6 cm, L_{TOT} = 41 cm and V_{TOT} = 200 mL) equipped with an air distributor device (flow rate of 142 N cm³ min⁻¹).

The photoreactor was irradiated by four UV lamps (Philips, nominal power: 8 W each) with a main emission peak at 365 nm or by four visible lamps (Philips, nominal power: 8 W each) with an emission in the range 400–650 nm. The lamps surrounded the photoreactor external surface and positioned at an equal distance from it (about 30 mm) in order to irradiate the volume of the solution uniformly.

The photon flux at reactor external surface, obtained through actinometrical technique [39,40] using a spectro-radiometer (StellarNet Inc), was about 25 and 26 mW cm⁻² for UV and visible lamps, respectively.

The photocatalyst dosage was 0.3 g in 100 mL aqueous solution containing an established concentration of dye. Continuous mixing of the solution in the reactor was assured by external recirculation of the suspension through a peristaltic pump (Watson Marlow). The suspension was left in dark conditions for 120 min to reach the adsorption-desorption equilibrium of dye on the photocatalysts surface, and then the photocatalytic reaction was initiated under UV or visible light up to 240 min.

In order to compare the effect of the dye initial concentration and the photocatalyst dosage, different values of these parameters were considered. Thus, the investigated initial concentrations of EBT or PB or the solution containing simultaneously the two dyes are listed in Section 2.1 while the catalysts dosages were 0.15, 0.3, 0.6 and 0.9 g. The pH of the solutions has not been changed and it was equal to about 6.5 for all the photocatalytic tests, corresponding to the spontaneous pH of the solutions containing the target dyes. During the tests, 4 mL of solution were withdrawn with a syringe

Table 1

List of prepared photocatalysts with their characteristics.

	Undoped ZnO	Pr-ZnO(0.12%)	Pr-ZnO(0.23%)	Pr-ZnO(0.46%)	Pr-ZnO(0.69%)
Pr theoretical loading [mol%]	0	0.12	0.23	0.46	0.69
Pr measured loading (XRF) [mol%]	0	0.11	0.25	0.45	0.72
Cristallite size [nm]	25	25	25	21	21
SSA [$\text{m}^2 \text{ g}^{-1}$]	5	5	5	7	7
Band gap [eV]	3.3	3.0	3.0	3.0	3.0

and then they were centrifuged to remove the catalysts powders before the concentration measurement.

2.4. Analytical measurements

To measure the dyes concentration, UV–Vis spectrophotometer (Evolution 201) was used analyzing the absorbance of EBT at the wavelength of 580 nm and of PB at the wavelength of 630 nm.

The TOC was measured by the high temperature combustion method on a catalyst ($\text{Pt-Al}_2\text{O}_3$) in a tubular flow microreactor operated at 680 °C, with a stream of hydrocarbon free air to oxidize the organic carbon [41,42].

3. Results and discussion

3.1. Characterization of the photocatalysts

All the photocatalysts were characterized by using different techniques and the obtained results are shown and discussed in the following.

3.1.1. XRF and SSA results

SSA value of the undoped ZnO (Table 1) was $5 \text{ m}^2 \text{ g}^{-1}$ and it did not change when Pr amount was increased up to 0.23 mol%. The higher value of SSA ($7 \text{ m}^2 \text{ g}^{-1}$) was obtained for a Pr content of 0.46 and 0.69 mol%.

The total content of Pr in the samples was measured by XRF (Table 1). In every case, the real Pr content well agreed to the theoretical Pr content indicating a good yield of the doping process.

3.1.2. X-ray diffraction (XRD)

ZnO based photocatalysts were subjected to X-ray diffraction analysis. Fig. 1a shows the XRD patterns of the undoped and Pr-ZnO samples. XRD patterns of undoped ZnO showed five peaks at 2θ 32.06°, 34.74°, 36.53°, 47.85° and 56.97°, respectively indexed to the (1 0 0), (0 0 2), (1 0 1), (1 0 2) and (1 1 0) planes of hexagonal wurtzite crystal structure [43]. The main peaks of ZnO was observed after the doping with Pr, and no signal due to praseodymium oxides was detected, indicating that, probably, Pr^{3+} have been introduced in ZnO lattice successfully [44]. Moreover, this last result pointed out that there was no change in the crystal structure upon Pr doping.

However, since the ionic radius of Pr^{3+} (1.01 Å) is much larger than that one of Zn^{2+} (0.74 Å) [44], the exchange between Pr^{3+} and Zn^{2+} should induce a change of the ZnO lattice parameters.

To confirm the possible substitution of Zn^{2+} by Pr^{3+} ions in Pr-ZnO, the XRD spectra of the samples have been analyzed in the range 30–38° (Fig. 1b). Diffraction values of (1 0 0), (0 0 2), and (1 0 1) planes showed a shift to lower angles in the case of Pr-ZnO compared with undoped ZnO, evidencing the successful doping of Pr^{3+} into the ZnO lattice [44].

The average crystallite sizes (CS) of the prepared samples were calculated using the peak at $2\theta \sim 36^\circ$ through the Debye–Sherrer's equation (Table 1).

The CS value of Pr-ZnO(0.12%) and Pr-ZnO(0.23%) was the same as undoped ZnO (25 nm). When the Pr content was increased up

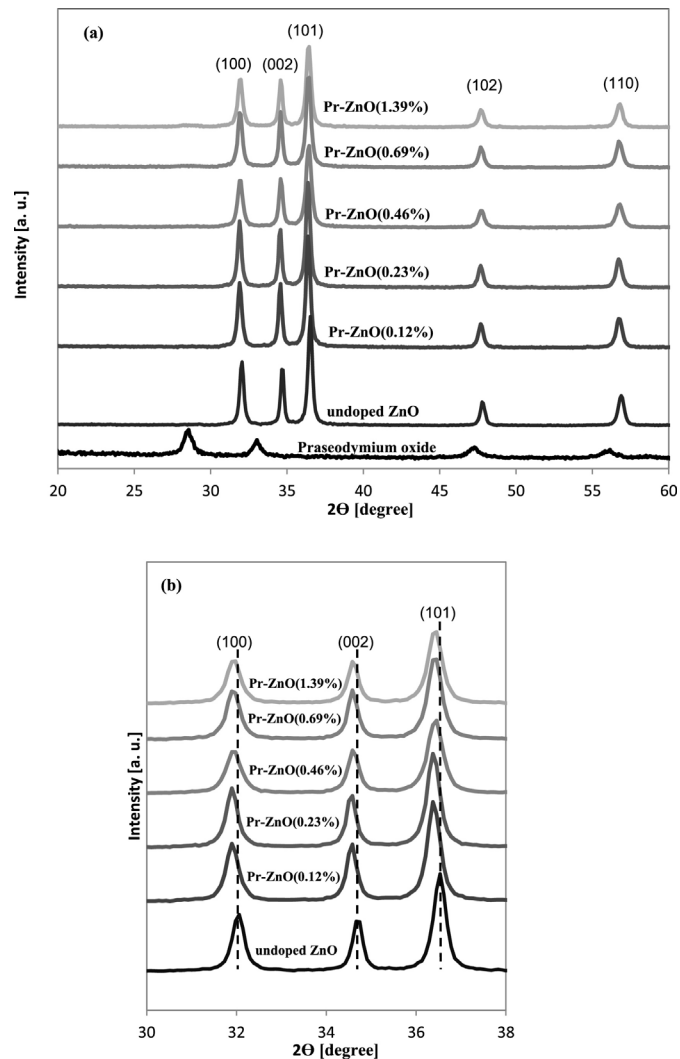


Fig. 1. (a) XRD patterns of undoped ZnO and Pr-ZnO photocatalysts in the range 20–60°; (b) XRD patterns of undoped ZnO and Pr-ZnO photocatalysts in the range 30–38°.

to 0.46 and 0.69 mol%, the CS decreased to 21 nm, while for further increase of Pr loading, the CS slightly increased (22 nm).

3.1.3. SEM analysis

Fig. 2 shows the SEM images of undoped and Pr-ZnO photocatalysts. For sake of brevity, together with undoped ZnO, only the analysis on Pr-ZnO at Pr loading of 0.46 and 1.39 mol% are reported, being similar the results obtained for all the others Pr-ZnO samples.

From the images it is possible to observe that both the undoped and Pr-ZnO samples are composed of a number of non-uniform macro aggregates. Therefore the doping process did not influence the overall morphology of the photocatalysts.

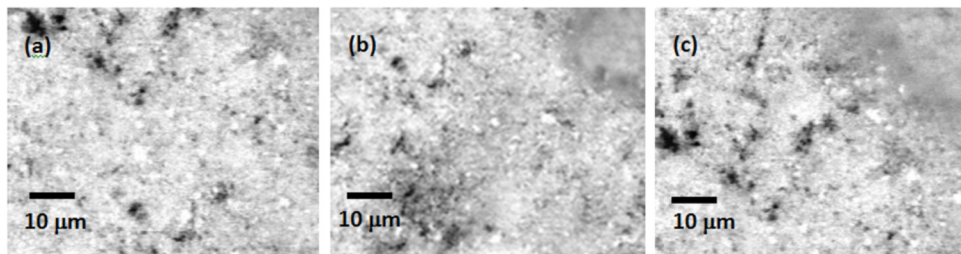


Fig. 2. SEM images (MAG 1.33kx) of undoped ZnO (a), Pr-ZnO(0.46%) (b) and Pr-ZnO(1.39%) (c).

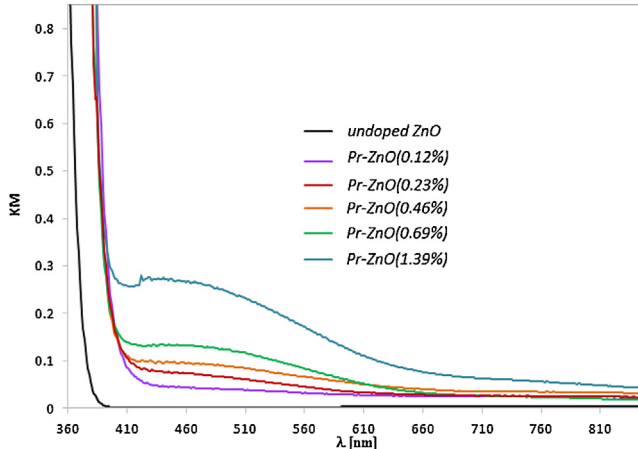


Fig. 3. UV-Vis diffuse reflectance spectra of undoped ZnO and Pr-ZnO photocatalysts.

3.1.4. UV-Vis diffuse reflectance spectra (UV-Vis DRS)

To study the optical absorption properties of the catalysts, UV-Vis DRS spectra in the range of 350–700 nm were investigated.

From Fig. 3, it is possible to observe that the absorption threshold of undoped ZnO is about 390 nm, assigned to the electron transition from O 2p to Zn 3d that corresponds to the transition from the valence band to the conduction band according to the energy band structure of ZnO [45].

On the contrary, the absorption edge of Pr-ZnO samples was red shifted toward the visible light region. This result underlines that the presence of Pr narrowed the band gap of doped photocatalysts [45], as shown in Table 1. The decrease of band gap energy from 3.3 eV of undoped ZnO up to 3.0 eV of doped samples can be attributed to the charge transfer between the ZnO valence or conduction band and Pr³⁺ 4f level [44,46,47] or to the formation of shallow level inside the band gap resulted from the Pr³⁺ ions incorporated into the ZnO lattice [44,46,48]. Moreover, Fig. 3 shows the presence of a wide absorption band in the range 410–660 nm for all Pr-ZnO samples that increased with the increase of Pr content. This wide spectral band in 410–660 nm could be probably ascribed to the f → f transition absorption and to the characteristic transition of Pr³⁺D₂ → H₄ [49,50], as previously observed for Pr-doped TiO₂ [49].

The Pr-ZnO samples indeed changed their color from pure white of the undoped ZnO to light pink (for the samples with the lower Pr content) up to light brown (for the highest Pr content).

3.1.5. Raman spectra

Fig. 4 shows the Raman spectra in the range 150–850 cm⁻¹ of the doped catalysts in comparison with undoped ZnO. In this range, there are four main bands at 331, 383, 438 and 583 cm⁻¹, related to the zinc oxide [27]. The strong and sharp band observed at 438 cm⁻¹ corresponds to the non polar optical phonons E2 (high) mode of ZnO. The features located at 331 and 383 cm⁻¹ correspond to the

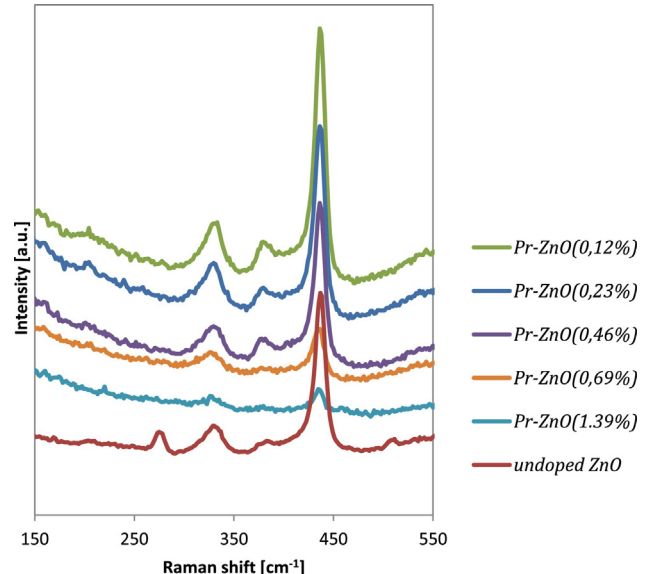


Fig. 4. Raman spectra of undoped ZnO and Pr-ZnO photocatalysts in the range 150–550 cm⁻¹.

multi-phonon scattering process E_{2H}–E_{2L} and A₁ (TO) phonons of ZnO crystal, respectively [51]. The signal located at 583 cm⁻¹ could be attributed to the E₁ (LO) feature, associated with the formation of defects such as oxygen vacancy [52]. No signals corresponding to praseodymium oxide were observed in the Raman spectrum of all the doped samples, confirming the results obtained from XRD analysis [53].

3.2. Adsorption of EBT in dark conditions

Adsorption of dyes on the surface of the catalyst is an important aspect in heterogeneous photocatalysis. Adsorption experiments in dark conditions were performed to determine the amount of EBT adsorbed (C*) on undoped ZnO and Pr-ZnO catalysts. Fig. 5 reports the behavior of C* as a function of the dye equilibrium concentration (C_{eq}) in aqueous solutions that was reached in 120 min of run time. It is possible to observe that, for all the doped samples, the C* value was always higher than that one obtained with undoped ZnO. It is very important to note that, the highest adsorption capacity was achieved with Pr-ZnO(0.46%) catalyst. Moreover the data reported in Fig. 5 evidenced that the behavior of C* as a function of C_{eq} was similar to Langmuir adsorption isotherm that can be modeled by the following equation:

$$\frac{C_{eq}}{C^*} = \frac{1}{b \cdot C_m} + \frac{1}{C_m} \cdot C_{eq} \quad (2)$$

where C_{eq} is the concentration of dye in the solution at equilibrium (mg L⁻¹), C* is the amount of EBT adsorbed (mg g⁻¹), C_m is

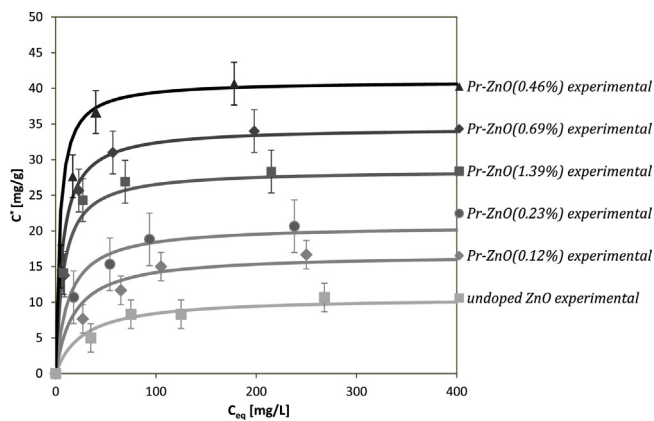


Fig. 5. EBT adsorption behavior as a function of EBT equilibrium concentration on undoped ZnO and Pr-ZnO photocatalysts; solution volume: 100 mL; catalyst dosage: 0.3 g.

the maximum adsorption capacity (mg g^{-1}) and b is the Langmuir adsorption equilibrium constant (L mg^{-1}).

The plot of C_{eq}/C^* as a function of C_{eq} gives a straight line where C_m and b can be derived, respectively, from the intercept and the slope of the obtained line.

The obtained values were shown in Table 2 evidencing that the values of b and C_m of Pr-ZnO samples were higher than that of the undoped ZnO. The enhanced adsorption capacity Pr-ZnO catalysts are induced by the change of the physical or chemical properties of the catalysts owing to Pr ion doping, as reported for Pr doped TiO₂ [49]. Moreover, it is reported that Pr³⁺ (or other lanthanide ions) could form chemical complexes with azo dyes [49,54,55], such as EBT, determining an increase of the adsorption capacity of EBT on Pr-ZnO in the aqueous suspension.

3.3. Photocatalytic activity results

3.3.1. Influence of Pr content

The photocatalytic activity of undoped ZnO and Pr-ZnO photocatalysts (catalyst amount: 0.3 g) was evaluated through the degradation of 100 mL of EBT at initial concentration of 100 mg L⁻¹ in the photoreaction apparatus (described in Section 2.3) under UV light. The results in terms of EBT discoloration as a function of irradiation time were illustrated in Fig. 6a. As it can be observed, there was an important decrease of the dye concentration during the irradiation time in the presence of all the prepared photocatalysts in comparison to the test without photocatalysts (photolysis test). A clear effect of Pr loading on the photocatalytic performances under UV light of undoped and Pr-ZnO catalysts can be established from the behavior of total organic carbon (TOC), shown in Fig. 6b. All the Pr-ZnO samples demonstrated higher photocatalytic performances than that of undoped ZnO. The photocatalytic activity of Pr-ZnO catalysts increased with the increase of Pr content until 0.46 mol% and then decreased when Pr content was higher than 0.69 mol%. It is worthwhile to note that, within 120 min of UV irradiation, Pr-ZnO(0.46%) allowed to achieve a TOC removal equal to about 94%, showing, therefore, the best photocatalytic performance under UV light.

To describe the degradation kinetics of EBT in the aqueous suspension, the Langmuir–Hinshelwood (L–H) kinetic model was applied. In fact, the L–H model is established based on Langmuir adsorption of the organic substrate onto the photocatalysts. Thus, the aspect of photocatalysts adsorption capacity is included in the L–H model [36]. The mathematical model has been realized considering that in the batch photoreactor under UV irradiation, occurred mainly the EBT discoloration and its mineralization.

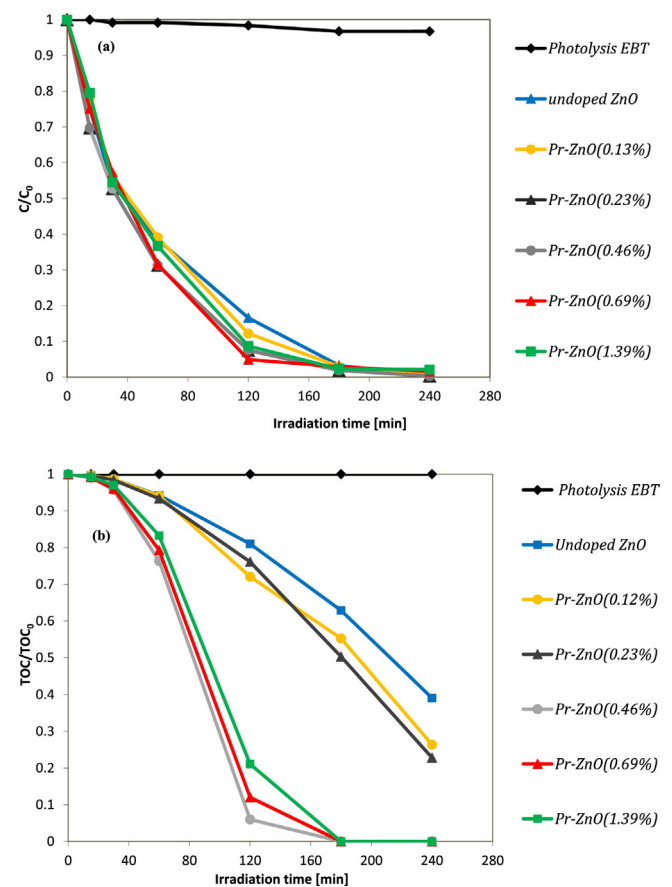


Fig. 6. (a) Photocatalytic EBT discoloration under UV light over undoped ZnO and Pr-ZnO catalysts; (b) Total Organic Carbon (TOC) behavior under UV light over undoped ZnO and Pr-ZnO photocatalysts; EBT initial concentration: 100 mg L⁻¹; solution volume: 100 mL; photocatalyst dosage: 0.3 g.

The L–H model, expressed in terms of EBT concentration and TOC content, are the following:

$$V \cdot \frac{dC}{dt} = -k \cdot C_m \cdot \frac{b \cdot C}{1 + b \cdot C} \cdot W_{\text{cat}} \quad (3)$$

$$V \cdot \frac{d\text{TOC}}{dt} = -k_c \cdot C_{m_c} \cdot \frac{b_c \cdot \text{TOC}}{1 + b_c \cdot \text{TOC}} \cdot W_{\text{cat}} \quad (4)$$

where dC/dt and $d\text{TOC}/dt$ are respectively the degradation and mineralization rate of EBT ($\text{mg L}^{-1} \text{ min}^{-1}$); k and k_c are the kinetic constants (min^{-1}) for EBT discoloration and TOC removal; W_{cat} is the weight of catalysts (g); V is the solution volume (L); C_m is the maximum amount of EBT adsorbed (mg g^{-1}) and b (L mg^{-1}) is the Langmuir adsorption equilibrium constant evaluated with Langmuir adsorption model (Table 2).

b_c (L mg^{-1}) and C_{m_c} used in Eq. (4) are defined according to the following relationships:

$$b_c = \frac{b \cdot PM_{\text{EBT}}}{n_c \cdot PM_c} \quad (5)$$

$$C_{m_c} = \frac{C_m}{n_c \cdot PM_c} \quad (6)$$

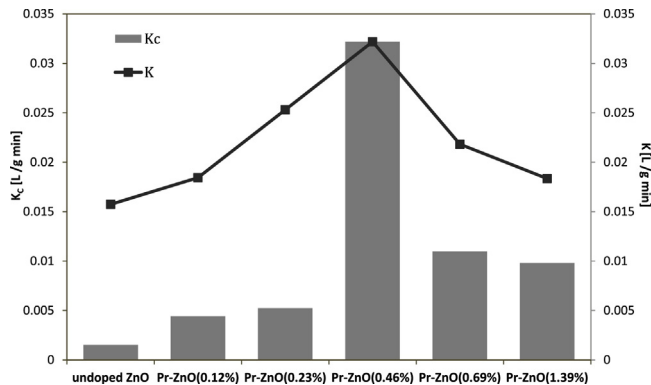
where PM_{EBT} is the molecular weight of EBT dye, PM_c is the molecular weight of carbon and n_c is the number of carbon atoms contained in the EBT molecule.

The obtained values for b_c and C_{m_c} of all the photocatalysts were reported in Table 2.

Table 2

Adsorption parameters evaluated with Langmuir adsorption model.

Photocatalysts		Undoped ZnO	Pr-ZnO(0.12%)	Pr-ZnO(0.23%)	Pr-ZnO(0.46%)	Pr-ZnO(0.69%)	Pr-ZnO(1.39%)
b	[L mg ⁻¹]	9.14×10^{-3}	9.68×10^{-3}	1.61×10^{-2}	3.30×10^{-2}	4.50×10^{-2}	6.33×10^{-2}
C_m	[mg g ⁻¹]	24.57	28.65	34.97	50.25	37.59	33.90
b_c	[L mg ⁻¹]	7.11×10^{-2}	1.06×10^{-1}	1.50×10^{-1}	4.81×10^{-1}	2.88×10^{-1}	2.50×10^{-1}
C_{m_c}	[mg g ⁻¹]	5.58	8.70	10.81	21.33	17.95	14.87

**Fig. 7.** Apparent kinetic constants for EBT discoloration and mineralization using undoped ZnO and Pr-ZnO photocatalysts under UV light; solution volume: 100 mL; EBT initial concentration: 100 mg L⁻¹; photocatalyst dosage: 0.3 g.

Eqs. (3) and (4) can be rearranged as follows:

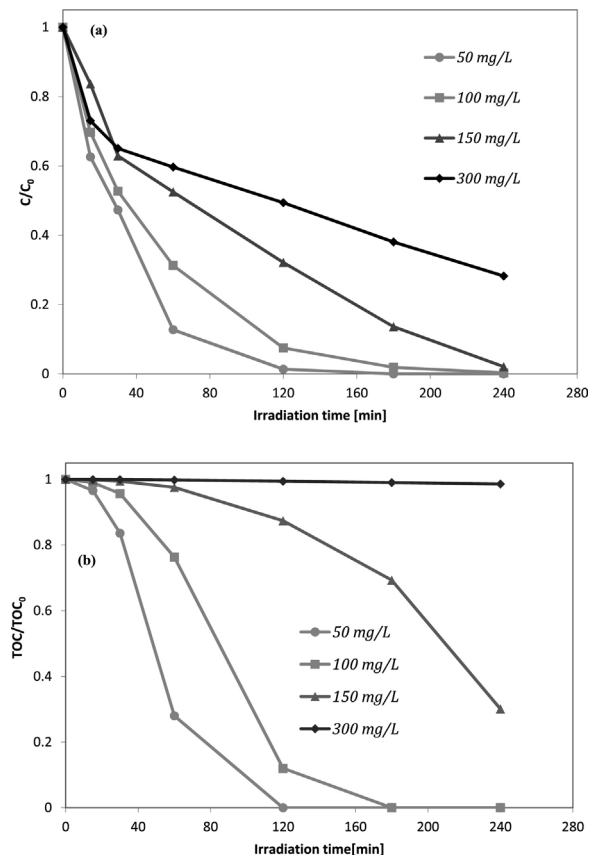
$$V \cdot \frac{dC}{dt} = -K \cdot \frac{C}{1 + b \cdot C} \cdot W_{\text{cat}} \quad (7)$$

$$V \cdot \frac{d\text{TOC}}{dt} = -K_c \cdot \frac{\text{TOC}}{1 + b_c \cdot \text{TOC}} \cdot W_{\text{cat}} \quad (8)$$

where K and K_c are the apparent rate constants ($\text{L min}^{-1} \text{g}^{-1}$) of EBT discoloration and mineralization, respectively, obtained by the following equations:

$$K = k \cdot C_m \cdot b \quad (9)$$

$$K_c = k_c \cdot C_{m_c} \cdot b_c \quad (10)$$

The initial conditions of Eqs. (7) and (8) are: $t = 0$, $C(t) = C_0$, $\text{TOC}(t) = \text{TOC}_0$ where C_0 and TOC_0 are the EBT concentration and TOC value after the dark phase.Eqs. (7) and (8), together with the initial conditions, were solved by the Euler iterative method allowing to identify the constants K and K_c by fitting experimental data reported in Fig. 6a and b as a function of UV irradiation time. The fitting procedure was realized by using the least squares approach. The obtained results were reported in Fig. 7. The highest values for K and K_c were obtained for Pr-ZnO(0.46%) photocatalyst. Moreover the results reported in Fig. 7 evidenced the existence of an optimal Pr loading. It is well known that the photocatalytic activity is attributed to both of the adsorption of organic substrate and the photocatalytic reaction [49]. The smaller crystallite size of the doped samples and the Pr^{3+} complex effect of the Pr-ZnO catalysts could be favorable for the better EBT adsorption enhancing, consequently, the photocatalytic activity [49].The presence of an optimum value for Pr content could be explained considering the XRD results (Fig. 1) in which it was underlined that the Pr^{3+} substituted Zn^{2+} . This phenomenon caused an electric charge imbalance, as previously observed for Pr-doped TiO_2 [56]. Possibly, in order to compensate this charge imbalance, more hydroxide ions may be adsorbed on the ZnO surface determining the enhanced photocatalytic activity of Pr-ZnO samples. Moreover, the ZnO lattice distortion generated by the doping could**Fig. 8.** (a) Photocatalytic EBT discoloration under UV light at different initial dye concentration on Pr-ZnO(0.46%); (b) Total Organic Carbon (TOC) behavior under UV light at different initial dye concentration on Pr-ZnO(0.46%); solution volume: 100 mL; photocatalyst dosage: 0.3 g.reduce the recombination probability of electron-hole and thus improved both the EBT photocatalytic discoloration and mineralization [56]. This may happen when the Pr content was increased up to 0.46 mol%. When the doping level was further increased, the Pr^{3+} could become electron-hole recombination centers [49,56,57], thereby the recombination of the photogenerated electron-hole pairs becomes easier leading to the decreased photocatalytic activity.

Once obtained the optimal content of doping in ZnO lattice, to analyze the influence of operating conditions, additional photocatalytic activity tests were carried out by varying the dye concentration in solution and the dosage of Pr-ZnO(0.46%) photocatalyst.

3.3.2. Influence of EBT initial concentration in aqueous solution

The effect of initial EBT concentration on the photocatalytic activity of Pr-ZnO(0.46%) was studied in the range from 50 to 300 mg L⁻¹ while the other experimental conditions were unchanged.

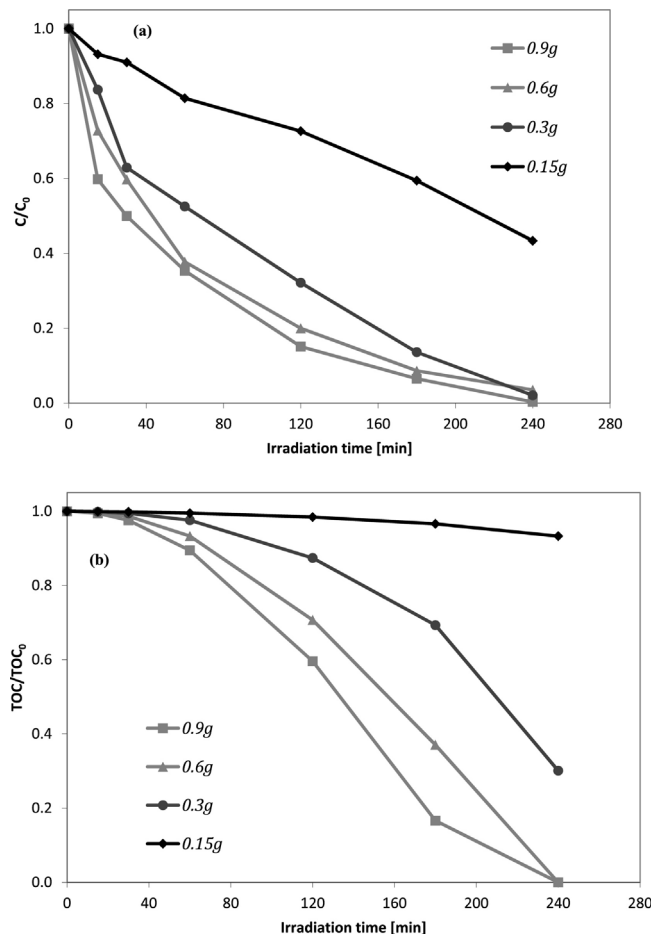


Fig. 9. (a) Photocatalytic EBT discoloration under UV light at different Pr-ZnO(0.46%) dosage; (b) Total Organic Carbon (TOC) behavior under UV light at different Pr-ZnO(0.46%) dosage; solution volume: 100 mL; EBT initial concentration: 100 mg L⁻¹.

Fig. 8a and **b** show, respectively, the EBT discoloration and TOC removal under UV light irradiation. Considering the initial EBT concentration at 50 mg L⁻¹, the total discoloration of the solution was achieved after 120 min. This last result was better than the data reported in literature obtained on nano ZnO at initial EBT dye concentration (46 mg L⁻¹) and photocatalyst amount (0.3 g) similar to those ones used in this paper [58].

From **Fig. 8a** and **b**, it can be noted that the photocatalytic activities gradually decreased with the increase of dye concentration in solution. This may be explained by the fact that the photonic flow was mitigated when the EBT concentration in solution was increased or rather the photons were intercepted before they can reach the catalyst surface, hence the absorption of photons by the catalyst photoactive surface decreased, and consequently the photocatalytic process is reduced [59].

So, to overcome this problem, photocatalytic tests at different amount of Pr-ZnO(0.46%) photocatalyst were performed.

3.3.3. Influence of Pr-ZnO(0.46%) dosage

The effect of Pr-ZnO(0.46%) dosage was evaluated in the range 0.15–0.9 g with an initial EBT concentration of 150 mg L⁻¹ and the results in terms of EBT discoloration and TOC removal were illustrated in **Fig. 9a** and **b**, respectively. It is possible to observe that the photocatalytic performances gradually improved with the increase of Pr-ZnO(0.46%) dosage. The complete mineralization of target dye was reached only when the amount of photocatalyst was higher than 0.3 g (**Fig. 9b**).

Table 3

Apparent kinetic constants for EBT discoloration (K) and mineralization (K_c) under UV light at different amounts of Pr-ZnO(0.46%) photocatalyst; solution volume: 100 mL; EBT initial concentration: 100 mg L⁻¹.

Pr-ZnO(0.46%) amount (g)	K (L g ⁻¹ min ⁻¹)	K_c (L g ⁻¹ min ⁻¹)
0.15	$(1.8 \pm 0.02) \times 10^{-3}$	$(3.7 \pm 0.1) \times 10^{-2}$
0.3	$(2.1 \pm 0.01) \times 10^{-2}$	$(6.6 \pm 0.09) \times 10^{-2}$
0.6	$(1.8 \pm 0.03) \times 10^{-2}$	$(5.8 \pm 0.15) \times 10^{-2}$
0.9	$(1.7 \pm 0.02) \times 10^{-2}$	$(3.2 \pm 0.09) \times 10^{-2}$

Table 4

EBT discoloration and TOC removal after 90 min of UV irradiation on Pr-ZnO(0.46%) photocatalyst for four cycles; solution volume: 100 mL; EBT initial concentration: 100 mg L⁻¹.

	1 cycle	2 cycle	3 cycle	4 cycle
Discoloration [%]	87 ± 2	89 ± 2	89 ± 2	88 ± 2
TOC removal [%]	84 ± 2	85 ± 2	87 ± 2	87 ± 2

To better understand the influence of Pr-ZnO(0.46%) dosage, it were estimated the values of K and K_c for the different amounts of photocatalyst used in the test (**Table 3**).

Both photocatalytic discoloration and mineralization increased when the photocatalyst amount was increased up to 0.3 g, indicating that the addition of more Pr-ZnO(0.46%) particles enhanced the number of the photoactive sites in the solution [60].

When the load of Pr-ZnO(0.46%) was increased from 0.6 to 0.9 g, the photocatalytic performances decreased due to an increase in the turbidity of the suspension and a decrease in UV light penetration as a result of increased scattering effect [37,59,61–63].

3.3.4. Stability experiments on Pr-ZnO(0.46%) photocatalyst

With the purpose to evaluate the photostability of the Pr-ZnO(0.46%) photocatalyst, recycle experiments under UV light irradiation were performed for four cycles with the same sample and experimental conditions. After reacting for 90 min, the photocatalyst were separated and washed several times with distilled water, after which it was dispersed into a fresh aqueous solution of EBT. After four recycling tests, Pr-ZnO(0.46%) sample didn't exhibit significant loss in activity and the EBT discoloration and TOC removal remained about 88 and 87%, respectively (**Table 4**). These results indicate that Pr-ZnO(0.46%) sample is a stable photocatalyst confirming the reproducibility of the photocatalytic process in the treatment of aqueous solutions containing high dye concentration.

3.3.5. EBT photodegradation under visible light

Fig. 10 reports the photocatalytic activity of undoped ZnO and Pr-ZnO(0.46%) under visible light with the EBT initial concentration of 100 mg L⁻¹ and with an amount of photocatalyst equal to 0.3 g. It was evident the inefficiency of undoped ZnO in comparison to the doped sample. On the contrary, the Pr-ZnO(0.46%) photocatalyst was able to degrade the target dye reaching a discoloration degree of 41% after 240 min of irradiation. The photocatalytic activity of the doped catalyst under visible light could be due to the transitions of 4f electrons of Pr³⁺ and to the red shift of the optical absorption edge of this sample [49], as observed from UV-Vis results (**Fig. 3**).

Moreover, the band gap energy value of undoped ZnO (3.3 eV) explains the inefficiency of this sample under visible light and exclude the ZnO sensitization phenomena that typically occur in the photocatalytic treatment of dyes with undoped semiconductors [64,65].

3.3.6. Influence of dye type

In order to evaluate the efficiency of Pr-ZnO(0.46%) photocatalyst with a different class of dye, a photocatalytic test has been carried out using an aqueous solution containing the food dye

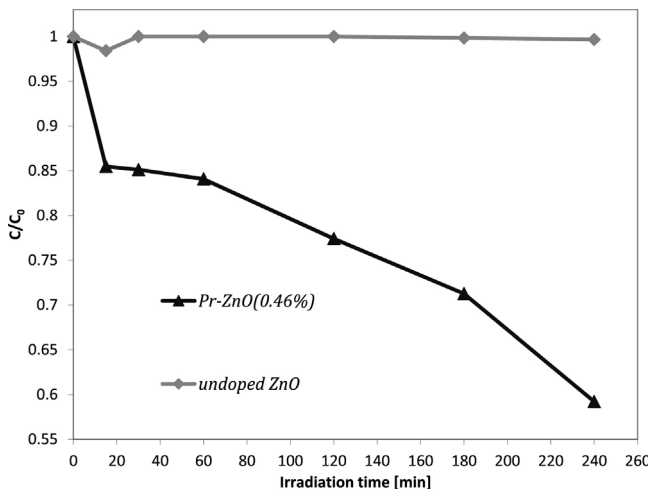


Fig. 10. Comparison of photocatalytic activities of undoped ZnO and Pr-ZnO(0.46%) photocatalyst under visible light; solution volume: 100 mL; EBT initial concentration: 100 mg L⁻¹; photocatalyst dosage: 0.3 g.

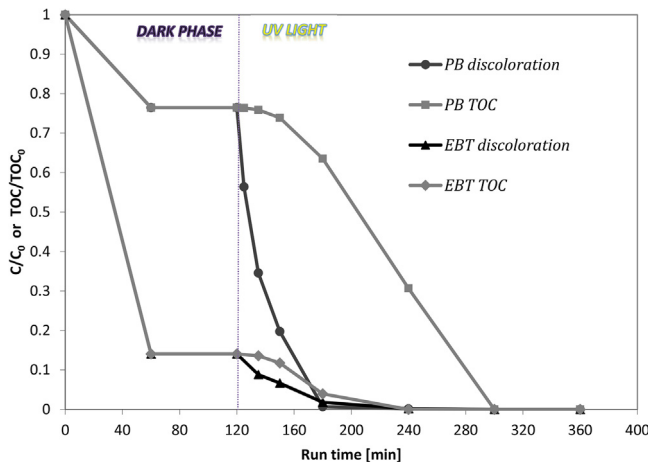


Fig. 11. Comparison between the discoloration and mineralization as a function of run time for the solution containing EBT or PB on Pr-ZnO(0.46%) under UV irradiation; solution volume: 100 mL; EBT or PB initial concentration: 50 mg L⁻¹; photocatalyst dosage: 0.3 g.

Patent Blue V (PB). With respect to EBT, which is an azo-dye, PB is a triphenylmethane dye.

Fig. 11 presents the comparison between the discoloration and mineralization of the dyes as a function of run time for an aqueous solution containing 50 mg L⁻¹ of EBT or 50 mg L⁻¹ of PB. The photocatalytic test was conducted under UV light with 0.3 g of Pr-ZnO(0.46%) sample. For both EBT and PB, in dark conditions the adsorption equilibrium on Pr-ZnO(0.46%) surface was reached in 60 min of the test. It is possible to observe that the adsorption amount was much higher for EBT dye (about 86%) than PB dye (about 24%), demonstrating the much higher affinity of the Pr-ZnO(0.46%) photocatalyst toward the EBT dye, specifically, and toward the azo-dyes, generally, with respect to triphenylmethane dyes, such as PB.

Moreover, under UV light, the complete discoloration of both dyes was achieved after 60 min of irradiation time, while the total TOC removal was reached after 120 and 180 min of irradiation time for EBT and PB, respectively. The different mineralization behavior could be correlated to the different chemical structure of EBT and PB dyes [66]. As shown by experimental data in dark conditions (Fig. 11), the adsorptive affinity of EBT on Pr-ZnO(0.46%) was higher than PB; therefore photocatalytic activity is faster for EBT.

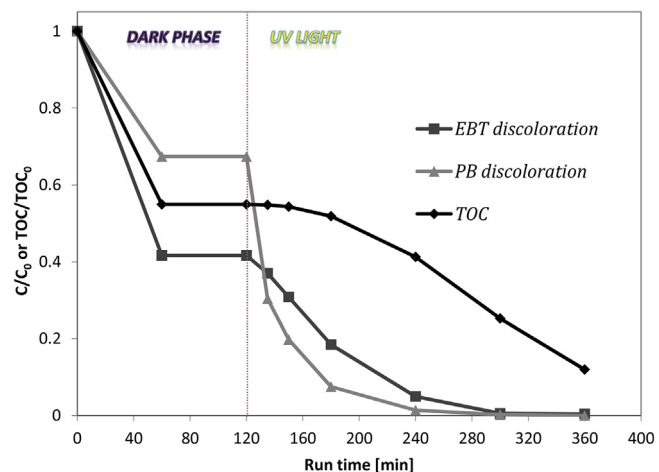


Fig. 12. Discoloration and TOC removal of the binary mixture solution of EBT and PB as a function of run time on Pr-ZnO(0.46%) under UV irradiation; solution volume: 100 mL; EBT and PB initial concentration: 50 mg L⁻¹; photocatalyst dosage: 0.3 g.

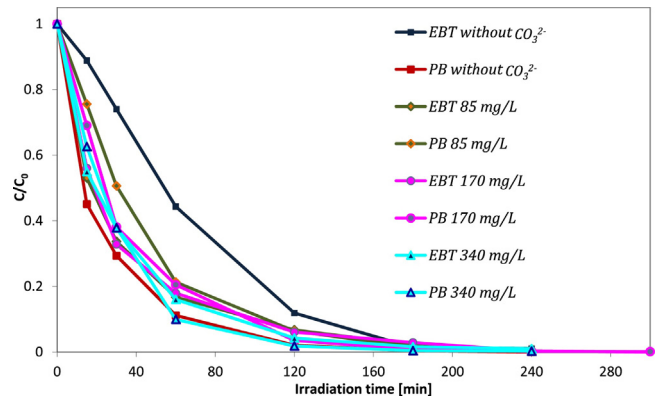


Fig. 13. Influence of carbonate ions in the photocatalytic discoloration of binary mixture solution of EBT and PB on Pr-ZnO(0.46%) photocatalyst under UV irradiation; solution volume: 100 mL; EBT and PB initial concentration: 50 mg L⁻¹; photocatalyst dosage: 0.3 g.

It is worthwhile to note that most of the photocatalytic studies have been done based on single dye solution [22,36,37,67]. However, industrial effluents contain a mixture of dyes. So, there is a need to study the photocatalytic treatment of a mixture of dyes.

Fig. 12 shows the discoloration and TOC reduction, as a function of run time, of a binary mixture solution of EBT and PB in equal concentration (50 mg L⁻¹) using Pr-ZnO(0.46%) photocatalyst. In dark conditions, also for the binary mixture of the two dyes, the amount of EBT adsorbed was higher than that achieved for PB dye. Under UV light, the obtained results evidenced that the complete discoloration of the solution was achieved after 180 min of UV irradiation, while after 240 min, the TOC removal was 88% highlighting that the optimized photocatalyst was able to efficiently treat a complex solution containing more dyes simultaneously.

3.3.7. Influence of carbonate ions on photocatalytic activity

In this study, the effect of ions scavengers such as carbonate ions (CO₃²⁻) on the photocatalytic activity of Pr-ZnO(0.46%) was investigated. Hence, photocatalytic tests have been carried out with CO₃²⁻ concentration in the range 85–340 mg L⁻¹ in the binary mixture of the two dyes. The results in terms of discoloration as a function of irradiation time were presented in Fig. 13. For the tests, it was prepared the dyes mixture with the addition of sodium carbonate (Na₂CO₃).

Table 5

TOC removal in the presence of carbonate ions for the binary mixture dyes solution under UV irradiation using Pr-ZnO(0.46%); solution volume: 100 mL; EBT and PB initial concentration: 50 mg L⁻¹; photocatalyst dosage: 0.3 g.

TOC removal [%]	CO ₃ ²⁻ [mg L ⁻¹] Without CO ₃ ²⁻	85 (mg L ⁻¹)			170 (mg L ⁻¹)		340 (mg L ⁻¹)	
		70 ± 5	77 ± 5	82 ± 5	76 ± 5			

Na₂CO₃ is a common auxiliary chemical used in textile processing operations. It has an important role in the dye fixing and in the fastness of color on the textiles [21]. For this reason, the wastewater from the dyeing operation could contain considerable amount of CO₃²⁻ and so, it is important to understand the influence of carbonate ions in the treatment efficiency. Fig. 13 shows that the photocatalytic activities of Pr-ZnO(0.46%) were slightly improved in the presence of CO₃²⁻ also with a very high concentration of carbonate ions (about 340 mg L⁻¹). In other studies, it was found that the presence of carbonate implies an enhancement of the photocatalytic performance of ZnO [17] even if carbonate ions are a well-known interfering agent which, generally, produce a significant reduction in the photocatalytic processes. The enhancement of the photocatalytic efficiency in the presence of CO₃²⁻ could involve the formation of carbonate radical by direct reaction between carbonate and the photogenerated holes (h⁺) [17]. The carbonate radicals could react with dyes molecules present in the bulk solution. This phenomenon, coupled with the action of the hydroxyl radicals that react with the previously adsorbed dyes molecules [17], contributed to enhance the overall photocatalytic discoloration performances observed for Pr-ZnO(0.46%) photocatalyst.

Finally, the presence of CO₃²⁻ didn't influence the TOC removal that reached a value of about 80% after 240 min of UV irradiation (Table 5).

3.3.8. Application of the photocatalytic system for the treatment of a real wastewater

The photocatalytic performances of Pr-ZnO(0.46%) photocatalyst on a real industrial wastewater containing the Basic Red 51 (BR51) dye was also investigated in this study.

BR51 is a soluble dye belonging to the azo-dye class that is largely used in many commercial formulations for semipermanent hair dyeing [68]. A lot of the compounds and derivatives present in coloring formulations are issued in the environment and in particular through industrial wastewater. In this sense, Annex III of the EU Cosmetic Directive has limited the concentrations of hair dyes in hair coloring formulations and has prohibited the presence of particular substances in these products [68]. Dyeing hair wastewater samples were collected from a dyeing hair industry. The main physicochemical parameters of the wastewater are: TOC = 900 mg L⁻¹, pH = 6.5 and CO₃²⁻ = 156 mg L⁻¹. The concerned industrial wastewater presents a brilliant pink color as shown in Fig. 14a.

The photocatalytic experiments were carried with 100 mL of wastewater under UV light irradiation. The results were shown in Fig. 14a where the discoloration of the real wastewater was determined from the monitoring of the absorbance (A) at $\lambda_{\text{max}} = 524 \text{ nm}$ (due to the azo chromophore group of BR51 dye) using Evolution 201 UV-Vis spectrophotometer. It can be observed that, in dark conditions, a discoloration and a TOC reduction of about 52 and 30%, respectively was achieved after 120 min (Fig. 14a) due to the adsorption phenomena in presence of the photocatalyst. Under UV light, the total discoloration with the almost complete mineralization of the organic content was reached after 360 min of irradiation time (Fig. 14a). For visual comparison, photos of the sample of dyeing hair wastewater before (Fig. 14b) and after the photocatalytic test (Fig. 14c) are also shown.

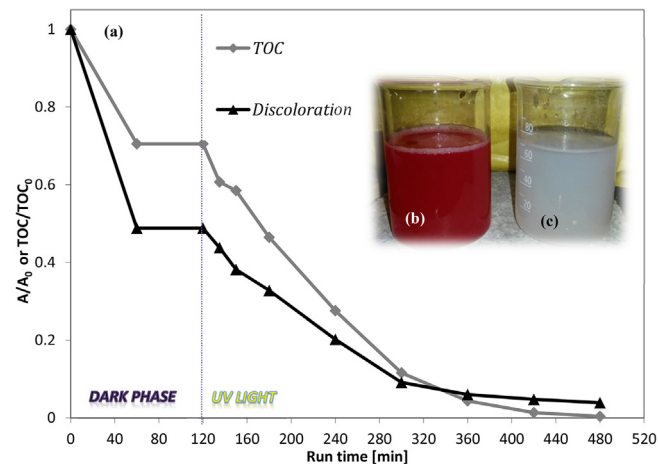


Fig. 14. (a) Discoloration and TOC behavior of a real industrial wastewater using Pr-ZnO(0.46%) photocatalyst under UV irradiation; solution volume: 100 mL; photocatalyst dosage: 0.3 g; absorbance band (A): 529 nm; (b) Dyeing hair wastewater before photocatalytic test; (c) Dyeing hair wastewater after photocatalytic test.

Finally, it has been performed a photocatalytic experiment in presence of visible light (not shown) whose results evidenced a discoloration degree and TOC removal of about 60 and 30%, respectively, after 240 min of irradiation time.

These results confirm the applicability of the photocatalytic process also to a real wastewater using an optimized Pr-ZnO photocatalyst active both under UV light and visible light irradiation.

4. Conclusions

In this work the photocatalytic activity of Pr-doped ZnO photocatalysts has been addressed for the first time in the treatment of aqueous solutions at high concentration of organic dyes under UV or visible light irradiation. The prepared photocatalysts have been characterized by different techniques evidencing that ZnO is present as hexagonal wurtzite phase and that Pr³⁺ ions were successfully incorporated into the ZnO lattice. Moreover, Pr-ZnO samples present band-gap values of about 3.0 eV, lower than undoped ZnO (3.3 eV). The highest enhancement in the photocatalytic activity under UV light was achieved using ZnO doped with 0.46 mol% of Pr, named Pr-ZnO(0.46%). In fact, after 120 min of UV irradiation, the complete removal of the azo dye Eriochrome Black T (EBT) was achieved. The photoactivity improvement may be correlated to the ZnO lattice distortion generated by the doping with Pr³⁺ that could inhibit the recombination probability of the photogenerated electron-hole pair, thus improving both the EBT photocatalytic discoloration and mineralization. Moreover, the smaller crystallite size of Pr-ZnO(0.46%) and the Pr³⁺ complex effect on the Pr-ZnO catalysts could be favorable for the better EBT adsorption enhancing, consequently, the photocatalytic activity.

Pr-ZnO(0.46%) sample showed a significant photocatalytic activity also under visible light while undoped ZnO was ineffective. The optimized photocatalyst was also able to remove a different type of dyes such as such as the triphenylmethane Patent Blue V (PB), demonstrating the efficiency of the photocatalytic system in the treatment of different dyes class. Good results were obtained

also on the photodegradation of a binary mixture solution of EBT and PB and it was observed that the presence of ions scavengers (carbonate ions) didn't inhibit the photocatalytic performances of the optimized photocatalyst. Finally, the complete discoloration and mineralization of Basic Red 51 dye present in a dying hair industrial wastewater, has been obtained after 360 min under UV light, confirming the efficiency of the optimized photocatalyst in the treatment of real wastewater at very high concentration of organic dyes.

Acknowledgment

PhD Olga Sacco thanks Thermotec SRL (Salerno) for the SEM analysis of the samples presented in the manuscript.

References

- [1] V. Misra, S.D. Pandey, Environ. Int. 31 (2005) 417–431.
- [2] B. Pal, R. Kaur, I.S. Grover, J. Ind. Eng. Chem. 33 (2016) 178–184.
- [3] J. Kaur, S. Singh, Superlattices Microstruct. 83 (2015) 9–21.
- [4] V. Vaiano, G. Iervolino, D. Sannino, L. Rizzo, G. Sarno, A. Farina, Appl. Catal., B: Environ. 160–161 (2014) 247–253.
- [5] V. Vaiano, O. Sacco, G. Iervolino, D. Sannino, P. Ciambelli, R. Liguori, E. Bezzeccheri, A. Rubino, Appl. Catal., B: Environ. 176–177 (2015) 594–600.
- [6] I. Seynure, F. Aliyev, M. Stoller, A. Chianese, Optimal configuration of a photocatalytic lab-reactor by using immobilized nanostructured TiO₂, Chem. Eng. Trans. 19 (2016) 199–204.
- [7] J.M. Ochando-Pulido, M. Stoller, Chem. Eng. J. 279 (2015) 387–395.
- [8] G. Carini Jr., F. Parrino, G. Palmisano, G. Scandura, I. Citro, G. Calogero, A. Bartolotta, G. Di Marco, Photochem. Photobiol. Sci. 14 (2015) 1685–1693.
- [9] M.A. Mahmood, S. Baruah, A.K. Anal, J. Dutta, Environ. Chem. Lett. 10 (2012) 145–151.
- [10] S.M. Lam, J.C. Sin, A.Z. Abdullah, A.R. Mohamed, Desalin. Water Treat. 41 (2012) 131–169.
- [11] A. Duta, M. Visa, J. Photochem. Photobiol., A 306 (2015) 21–30.
- [12] C. Gionco, D. Fabbri, P. Calza, M.C. Paganini, J. Nanomater. 2016 (2016) 7, Article ID 4129864 <http://dx.doi.org/10.1155/2016/4129864> 2016.
- [13] P. Calza, C. Gionco, M. Giletta, M. Kalaboka, V.A. Sakkas, T. Albanis, M.C. Paganini, J. Hazard. Mater. 323 (2017) 471–477.
- [14] C. Garlisi, G. Scandura, J. Szlachetko, S. Ahmadi, J. Sa, G. Palmisano, Appl. Catal., A: Gen. 526 (2016) 191–199.
- [15] Y. Abdel-Maksoud, E. Imam, A. Ramadan, Catalysts 6 (2016) 138–164.
- [16] Y. Chen, J.Y. Wang, W.Z. Li, M.T. Ju, Cailiao Gongcheng/J. Mater. Eng. 44 (2016) 103–113.
- [17] C.A. Gouveia, F. Wypych, S.G. Moraes, N. Duran, N. Nagata, P. Peralta-Zamora, Chemosphere 40 (2000) 433–440.
- [18] A.M. Abdulkarem, E.M. Elssfah, N.-N. Yan, G. Demissie, Y. Yu, J. Phys. Chem. Solids 74 (2013) 647–652.
- [19] F. Tian, Y. Liu, Scr. Mater. 69 (2013) 417–419.
- [20] X. Cai, Y. Cai, Y. Liu, H. Li, F. Zhang, Y. Wang, J. Phys. Chem. Solids 74 (2013) 1196–1203.
- [21] P. Peralta-Zamora, C.A.K. Gouveia, F. Wypych, N. Duran, Toxicol. Environ. Chem. 80 (2001) 83–93.
- [22] K.M. Lee, S.B. Abdul Hamid, C.W. Lai, Mater. Sci. Semicond. Process. 39 (2015) 40–48.
- [23] N. Elaziouti, B. Laouedj, J. Ahmed, Chem. Eng. Process. Technol. 2 (2011) 106.
- [24] S.-Y. Pung, W.-P. Lee, A. Aziz, Int. J. Inorg. Chem. 608183 (2012) 1–9.
- [25] S. Chakrabarti, B.K. Dutta, J. Hazard. Mater. 112 (2004) 269–278.
- [26] E. Yassitepe, H.C. Yatmaz, C. Öztürk, K. Öztürk, C. Duran, J. Photochem. Photobiol., A 198 (2008) 1–6.
- [27] M. Faisal, A.A. Ismail, A.A. Ibrahim, H. Bouzid, S.A. Al-Sayari, Chem. Eng. J. (Amsterdam, Netherlands) 229 (2013) 225–233.
- [28] A. Phuruangrat, O. Yayapao, T. Thongtem, S. Thongtem, J. Nanomater. 367529/367521–367529/367529 (2014) 367510.
- [29] N. Muhd Julkapli, S. Bagheri, S. Bee Abd Hamid, Sci. World J. 2014 (2014) 1–25.
- [30] N. Guy, M. Ozacar, Int. J. Hydrogen Energy 41 (2016) 20100–20112.
- [31] S. Kuriakose, B. Satpati, S. Mohapatra, Phys. Chem. Chem. Phys. 16 (2014) 12741–12749.
- [32] R. Gupta, N. KrishnaRao Eswar, J.M. Modak, G. Madras, RSC Adv. 6 (2016) 85675–85687.
- [33] X. Yu, D. Meng, C. Liu, K. Xu, J. Chen, C. Lu, Y. Wang, J. Mater. Sci.: Mater. Electron. 25 (2014) 3920–3923.
- [34] S. Dong, K. Xu, J. Liu, H. Cui, Physica B: Condens. Matter 406 (2011) 3609–3612.
- [35] T.M. Milao, V.R. de Mendonça, V.D. Araújo, W. Avansi, C. Ribeiro, E. Longo, M.I. Bernardi, Sci. Adv. Mater. 4 (2012) 54–60.
- [36] I. Kazeminezhad, A. Sadollahkhani, Mater. Lett. 120 (2014) 267–270.
- [37] V. Vaiano, G. Iervolino, D. Sannino, J.J. Murcia, M.C. Hidalgo, P. Ciambelli, J.A. Navío, Appl. Catal., B: Environ. 188 (2016) 134–146.
- [38] S.M. Twang, L.L. Zhi, M.A.A. Zaini, Q.Z. Yong, A.Y.P. Yee, Adv. Environ. Res. (Hauppauge, NY, U.S.) 36 (2015) 217–234.
- [39] S.E. Braslavsky, A.M. Braun, A.E. Cassano, A.V. Emeline, M.I. Litter, L. Palmisano, V.N. Parmon, N. Serpone, Pure Appl. Chem. 83 (2011) 931–1014.
- [40] H.J. Kuhn, S.E. Braslavsky, R. Schmidt, Pure Appl. Chem. 76 (2004) 2105–2146.
- [41] D. Sannino, V. Vaiano, L.A. Isupova, P. Ciambelli, J. Adv. Oxid. Technol. 15 (2012) 294–300.
- [42] D. Sannino, V. Vaiano, P. Ciambelli, L.A. Isupova, Chem. Eng. J. 224 (2013) 53–58.
- [43] O. Yayapao, T. Thongtem, A. Phuruangrat, S. Thongtem, Mater. Sci. Semicond. Process. 39 (2015) 786–792.
- [44] A. Khataee, A. Karimi, S. Arefi-Oskoui, C.S.R. Darvishi, Y. Hanifehpour, B. Soltani, S.W. Joo, Ultrason. Sonochem. 22 (2015) 371–381.
- [45] L. Zhang, Y. Yang, R. Fan, J. Yu, L. Li, J. Mater. Chem., A 1 (2013) 12066–12073.
- [46] V. Stengl, S. Bakardjieva, N. Murafa, Mater. Chem. Phys. 114 (2009) 217–226.
- [47] J.-C. Sin, S.-M. Lam, K.-T. Lee, A.R. Mohamed, Ceram. Int. 39 (2013) 5833–5843.
- [48] O. Yayapao, T. Thongtem, A. Phuruangrat, S. Thongtem, J. Alloys Compd. 576 (2013) 72–79.
- [49] C. Liang, C. Liu, F. Li, F. Wu, Chem. Eng. J. (Amsterdam, Netherlands) 147 (2009) 219–225.
- [50] C. Liang, H. Zhang, L. Jiang, D. Zhang, Fresenius Environ. Bull. 22 (2013) 3229–3235.
- [51] S. Guo, Z. Du, S. Dai, Condens. Matter 46 (2009) 2329–2332.
- [52] A. Janotti, C.G. Van de Walle, Rep. Prog. Phys. 72 (2009), 126501/126501/1126501.
- [53] P. Ilanchezhiyan, G.M. Kumar, M. Subramanian, R. Jayavel, Mater. Sci. Eng., B 175 (2010) 238–242.
- [54] F.B. Li, X.Z. Li, M.F. Hou, K.W. Cheah, W.C.H. Choy, Appl. Catal., A: Gen. 285 (2005) 181–189.
- [55] B. Yan, K. Zhou, J. Alloys Compd. 398 (2005) 165–169.
- [56] F. Huang, S. Wang, S. Zhang, Y. Fan, C. Li, C. Wang, C. Liu, Bull. Korean Chem. Soc. 35 (2014) 2512–2518.
- [57] X. Liu, J. Xing, J. Qiu, X. Sun, Indian J. Chem., Sect. A: Inorg., Bio-inorg., Phys., Theor. Anal. Chem. 52A (2013) 1257–1262.
- [58] J.A.P.M. Esther leena Preethi, S. Thiriveni, J. Appl. Chem. 8 (2015) 8.
- [59] M.A. Behnajady, N. Modirshahla, R. Hamzavi, J. Hazard. Mater. 133 (2006) 226–232.
- [60] L. Rizzo, D. Sannino, V. Vaiano, O. Sacco, A. Scarpa, D. Pietrogiamoni, Appl. Catal., B: Environ. 144 (2013) 369–378.
- [61] V. Vaiano, G. Iervolino, G. Sarno, D. Sannino, L. Rizzo, J.J. Murcia Mesa, M.C. Hidalgo, J.A. Navío, Oil Gas Sci. Technol. 70 (2015) 891–902.
- [62] I.K. Konstantinou, T.A. Albanis, Appl. Catal., B: Environ. 49 (2004) 1–14.
- [63] M. Pera-Titus, V. Garcia-Molina, M.A. Banos, J. Gimenez, S. Esplugas, Appl. Catal., B: Environ. 47 (2004) 219–256.
- [64] S. Singh, A. Singh, N. Kaur, Bull. Mater. Sci. 39 (2016) 1371–1379.
- [65] S. Namba, Y. Hishikiri, J. Phys. Chem. 69 (1965) 774–779.
- [66] V. Vaiano, O. Sacco, D. Sannino, P. Ciambelli, Appl. Catal., B: Environ. 170–171 (2015) 153–161.
- [67] S.K. Kansal, S. Sood, A. Umar, S.K. Mehta, J. Alloys Compd. 581 (2013) 392–397.
- [68] L.E. Fraga, J.H. Franco, M.O. Orlandi, M.V.B. Zanoni, J. Environ. Chem. Eng. 1 (2013) 194–199.